Japan Society of Histochemistry and Cytochemistry
Established 1959

Acta Histochem. Cytochem. 57 (2): 67–74, 2024
doi: 10.1267/ahc.23-00066

Regular Article

C-C Chemokine 21-Expressing T-cell Zone Fibroblastic Reticular Cells, Abundant in Lymph Nodes, Are Absent in Cancer Lymphoid Stroma

Haruo Ohtani[1,2], Kazuhiko Matsuo[3], Kosuke Kitahata[3,5], Eiichi Sato[4] and Takashi Nakayama[3]

[1]Departments of Pathology, Mito Saiseikai General Hospital, Mito, Japan , [2]Department of Pathology, Ibaraki Children Hospital, Mito, Japan , [3]Division of Chemotherapy, Kindai University Faculty of Pharmacy, Osaka, Japan , [4]Department of Pathology, Tokyo Medical University, Tokyo, Japan and [5]Present address: Laboratory for Immunological Memory, RIKEN Center for Integrative Medical Sciences, Yokohama, Japan

Received October 24, 2023; accepted February 9, 2024; published online April 4, 2024

Cancer tissue generally possesses an immunosuppressive microenvironment. However, some cancers are associated with lymphoid stroma (i.e., a widely developed tertiary lymphoid structure). The T-cell zone (paracortex) of secondary lymphoid organs, particularly lymph nodes, is characterized by an abundance of T-cell zone fibroblastic reticular cells (TCZ-FRCs) that express C-C motif chemokine ligand 21 (CCL21) and smooth muscle actin (SMA). We analyzed the presence of TCZ-FRCs in 30 cases of carcinomas with lymphoid stroma of the breast, stomach, colon, tongue, and skin. Immunohistochemistry corroborated the abundance of $CCL21^+$ SMA^+ TCZ-FRCs in the normal lymph nodes. In sharp contrast, all 30 carcinomas with lymphoid stroma displayed no $CCL21^+$ SMA^+ TCZ-FRCs despite the affluence of T cells. Real-time reverse transcription polymerase chain reaction confirmed a marked decrease in the messenger ribonucleic acid expression of CCL21 and its receptor C-C motif chemokine receptor 7 in cancer lymphoid stroma compared to that in lymph nodes. Next, we analyzed the T cell phenotypes. The cancer lymphoid stroma demonstrated an abundance of $CD3^+$ $CD62L^-$ memory-type T cells, in contrast to the presence of $CD3^+$ $CD62L^+$ naïve- and central memory T cells in the T cell zone of lymphoid tissues. Our data demonstrated the following: 1) Cancer lymphoid stroma lacked TCZ-FRCs with abundance of more activated T cells than in lymph nodes and 2) these were common phenomena in cancer lymphoid stroma irrespective of the histological types and organs involved.

Key words: cancer lymphoid stroma, tertiary lymphoid structure, fibroblastic reticular cell, CCL21, CD62L

I. Introduction

Due to recent progress in immunotherapy of cancer, much attention is focused on tumor-infiltrating lymphocytes (TILs), and methods for a standardization of histopathological assessment of TILs have been published for histopathologial report [8, 9, 18]. Carcinoma with lymphoid stroma, also known as lymphoepithelioma-like carcinoma is a rare histopathological variant of carcinoma in various organs and is characterized by the formation of a TIL-rich stroma, whose prognosis is usually favorable [5, 9, 15, 22]. We have histopathologically analyzed this variant of carcinoma from the perspective of host immune responses to carcinoma cells [11–14, 17]. In 2009, we used the term tertiary lymphoid tissue for the lymphoid stroma of gastric carcinoma due to its similarity to secondary lymphoid organs [11, Fig. 8]. Thereafter, the term tertiary lymphoid structure (TLS) was proposed. The importance of

Correspondence to: Haruo Ohtani, M.D., Department of Pathology, Mito Saiseikai General Hospital, 3-3-10 Futabadai, Mito 311-4198, Japan.
E-mail: 311serenity@gmail.com

Table 1. *List of cases of carcinomas with lymphoid stroma*

Organ	Histology	# of cases	Age range	M/F	UICC TNM							Subtype
					Tis	T1	T2	T3	T4	N0	N1	
breast	Medullary carcinoma or carcinomas with medullary features	11	39–80	0/11	0	10	1	0	0	7	3	triple negative, 9; HER2(+), one; HER(−) luminal B, 2.
stomach	Adenocacinoma[1)]	6	58–81	6/0	0	4	1	1	0	6	0	EBV(+), 5; EBV(−), one.
colon	Adenocacinoma[2)]	2	53, 65	1/1	0	2	0	0	0	2	0	
tongue	squamous cell car.[3)]	7	33–89	3/4	0	7	0	0	0	7	0	p16(+), one; p16(−), 5.
skin	squamous cell car.[3)]	4	70–98	3/1	1	3	0	0	0	4	0	
total	all cases with LYMPHOID stroma	30	33–98; mean 67; SD 15	13/17	1	26	2	1	0	27	3	

car., carcinoma; EBV, Epstein-Barr virus; HER2, human epidermal growth factor receptor 2
All cases are cM0.
1) All cases are poorly differentiated adenocarcinoma with lymphoid stroma.
2) All cases are differentiated adenocarcinoma with lymphoid stroma.
3) All cases are differentiated squamous cell carcinoma with lymphoid stroma.

TLS in patient prognosis and its therapeutic benefits have been extensively analyzed in the field of tumor immunology [20, 21].

The T cell zone (paracortex) of secondary lymphoid organs, particularly lymph nodes, is characterized by well-developed meshwork of T-cell zone fibroblastic reticular cells (TCZ-FRCs). TCZ-FRCs secrete the C-C motif chemokine ligand (CCL) 19 and CCL21 to recruit C-C motif chemokine receptor (CCR) 7-expressing lymphocytes, particularly naïve T cells and thus contribute to the control of T cell responses. TCZ-FRCs are considered one of the important constituent cells of the secondary lymphoid organs [2, 4, 5]. The cancer lymphoid stroma structurally resembles the secondary lymphoid tissue (i.e., TLS), and T cells are abundant in both tissues. Therefore, we aimed to analyze whether TCZ-FRCs are present in the lymphoid stroma of cancers in various organs including the breast (particularly, medullary carcinomas), stomach, colon, tongue, and skin. Herein, we describe how the cancer lymphoid stroma differs from the secondary lymphoid organs in terms of TCZ-FRCs.

II. Materials and Methods

Materials

The present study included 30 patients with carcinomas characterized by well-formed lymphocyte-rich stroma, including medullary carcinomas or carcinomas with medullary features of the breast (11 cases), poorly differentiated adenocarcinomas with lymphoid stroma of the stomach (6 cases), well differentiated adenocarcinomas with lymphoid stroma of the colon (2 cases) and well differentiated squamous cell carcinomas with lymphoid stroma of the tongue (7 cases) and skin (4 cases) (Table 1) (Supplementary Fig. S1). Although the organs or histology of carcinoma were various, the histological features of lymphoid stroma of them were common in all cases (Supplementary Fig. S1). The age range of the participants was 33–98 years (average: 66.7; standard deviation: 15.3). The male: female (M/F) ratio was 13/17. To control the cancer lymphoid stroma, we used lymph nodes (12 cases), vermiform appendices (2 cases), and Peyer's patches (2 cases). The lymph nodes were located in nine gastrointestinal, two mediastinal or retroperitoneal, and one cervical region. All patients of control tissues were different from patients with carcinomas with lymphoid stroma. The age range of the patients of control tissues was 9–81 (average 48.3, standard deviation, 24.8). The M/F ratio was 10/6.

Immunohistochemistry

Immunohistochemistry was performed using formalin-fixed, paraffin-embedded tissues (FFPE). For single immunohistochemistry, the Leica Bond-MAX system or Nichirei Simple staining system was used. The primary antibodies used were goat polyclonal anti-CCL21 antibody (R&D Systems) and mouse monoclonal anti-smooth muscle actin (SMA) antibody (clone αsm-1, Leica Biosystems). Double- and triple-labeling immunohistochemistry was performed manually using Fast Red, HistoGreen, and diaminobenzidine as chromogens. Details of the staining methods and sources of other antibodies are described in Supplementary Methods.

Lymphocyte quantification was manually performed using an eyepiece lattice and a 40× objective lens, as described previously [11, 14]. Lymphocytes were measured in five representative T-lymphocyte-rich areas of in cancer stroma in each case, and the results were expressed as the average number of cells per lattice (0.0625 mm^2). Cancer lymphoid stroma and T-cell-rich zone in lymphoid tissue in all cases showed nearly uniform staining patters. Therefore, we judged that we could avoid severe sampling bias. The quantified cases included nine breast, three stomach, two

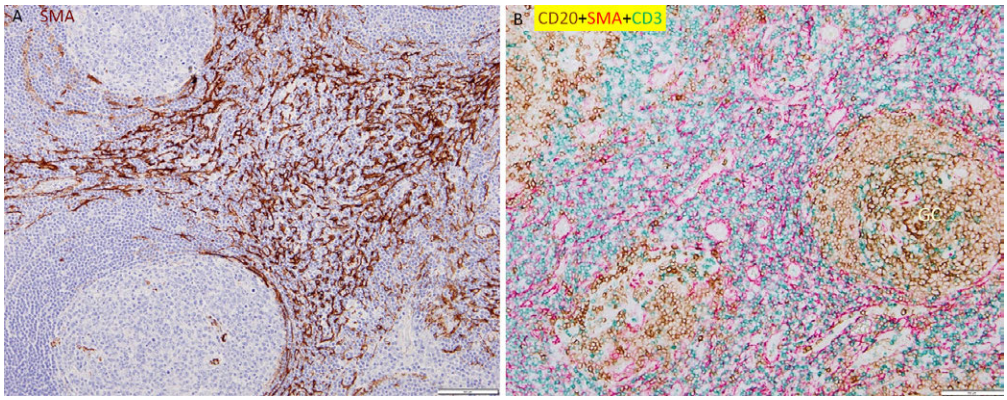

Fig. 1. Results in the T cell zone of the secondary lymphoid organs. **A**) Immunohistochemistry for SMA exhibiting an abundance of SMA^+ TCZ-FRCs in the T cell zone (paracortex) of normal lymph nodes. **B**) Triple immunostaining for CD20 (brown), SMA (Red), and CD3 (green) displays that the proliferation of SMA^+ TCZ-FRCs is confined within the $CD3^+$ T cell-rich T cell zone. GC, germinal center. Bars = 100 μm (**A**, **B**).

colon, seven tongue, and two skin cancers with lymphoid stroma. In the control group, seven lymph nodes, two vermiform appendices, and two Peyer patches were quantified.

Quantitative RT–PCR

Five to eight sections of 10–15 μm thickness were sliced from the FFPE blocks. The first slice was discarded to avoid contamination. Total RNAs were extracted from the FFPE tissue sections using PureLink FFPE Total RNA isolation Kit (Invitrogen Life Technologies, Carlsbad, CA). Total RNA (1 μg) was reverse-transcribed using the ReverTra Ace reverse transcription-quantitative polymerase chain reaction (RT qPCR) Master Mix (TOYOBO, Osaka, Japan). Quantitative real-time PCR was performed using the Thunderbird Probe qPCR Mix (TOYOBO) and the StepOne Real-Time PCR system (Applied Biosystems, Foster City, CA). The conditions for PCR were 95°C for 1 min, and then 40 cycles of 95°C for 15 sec (denaturation) and 60°C for 1 min (annealing extension). Primers and fluorogenic probes for CCL21 (Hs00171076_m1), CCL19 (Hs00355524_g1), CCR7 (Hs01013469_m1), and β2-microglobulin (Hs00984230_m1) were obtained from TaqMan Gene Expression Assays (Applied Biosystems). Gene expression was quantified using StepOne software (Applied Biosystems). To avoid sampling bias, we first confirmed that there were no significant differences in the expression levels of β2-microglobulin gene in the samples, and then we examined the expression of CCL21, CCL19, and CCR7.

III. Results

The secondary lymphoid organs abound with SMA^+ $CCL21^+$ T-cell zone fibroblastic reticular cells (TCZ-FRCs)

First, we corroborated that the T-cell zone (paracortex) of the secondary lymphoid organs, particularly the lymph nodes, exhibited a well-formed meshwork of TCZ-FRCs, as demonstrated by immunohistochemistry for SMA (Fig. 1A). Furthermore, triple staining for CD3, CD20, and SMA (performed in three cases) demonstrated that the TCZ-FRC meshwork was strictly located in the T cell zone (Fig. 1B). Double immunohistochemistry for CCL21 and SMA (performed in three cases) demonstrated that CCL21 and SMA were well colocalized in TCZ-FRCs (Supplementary Fig. S2A). Moreover, $CCL21^+$ TCZ-FRCs were different from mature dendritic cells that were identified by the expression of dendritic cell lysosome-associated membrane protein (DC-LAMP) (Supplementary Fig. S2B).

Cancer lymphoid stroma is uniformly devoid of TCZ-FRCs irrespective of histological types or organs

Cancers with lymphoid stroma are defined as cancers in which the majority of stroma comprises densely distributed lymphocytes (mainly T cells) with occasional formation of lymphoid follicles with germinal centers (mainly B cells) (details of HE features in Supplementary Fig. S1). In other words, lymphoid stroma corresponds 70–95% stromal TILs [8, 9] in wide areas of cancer stroma. Desmoplastic stroma was not observed or only focally observed. As described in the Materials, we analyzed 30 patients with breast, stomach, skin, tongue and colon carcinomas with lymphoid stroma (Table 1). Note that most cases are not in an advanced state. In all cases examined, the cancer lymphoid stroma was in sharp contrast to the lymph nodes, uniformly devoid of TCZ-FRCs, despite the abundance of T-cells in the areas. The aforementioned results were confirmed by single immunohistochemistry for CCL21 or SMA (performed in all 30 cases) (Fig. 2A, B) and double staining for CCL21 and SMA (performed in 25 cases) (Supplementary Fig. S2C). The abundance of T-cells without TCZ-FRCs was confirmed by triple staining for CD3, CD20, and CCL21 (performed in eight cases) (Fig. 2C). Additionally, CCL21 was observed in the vessels (Fig. 2A, B), which were identified as lymphatic vessels but not blood vessels, by triple staining for CD34, podoplanin (D2-40), and CCL21 (performed in 12 cases) (Fig. 2D). The confinement of CCL21 expression in lymphatic vessels

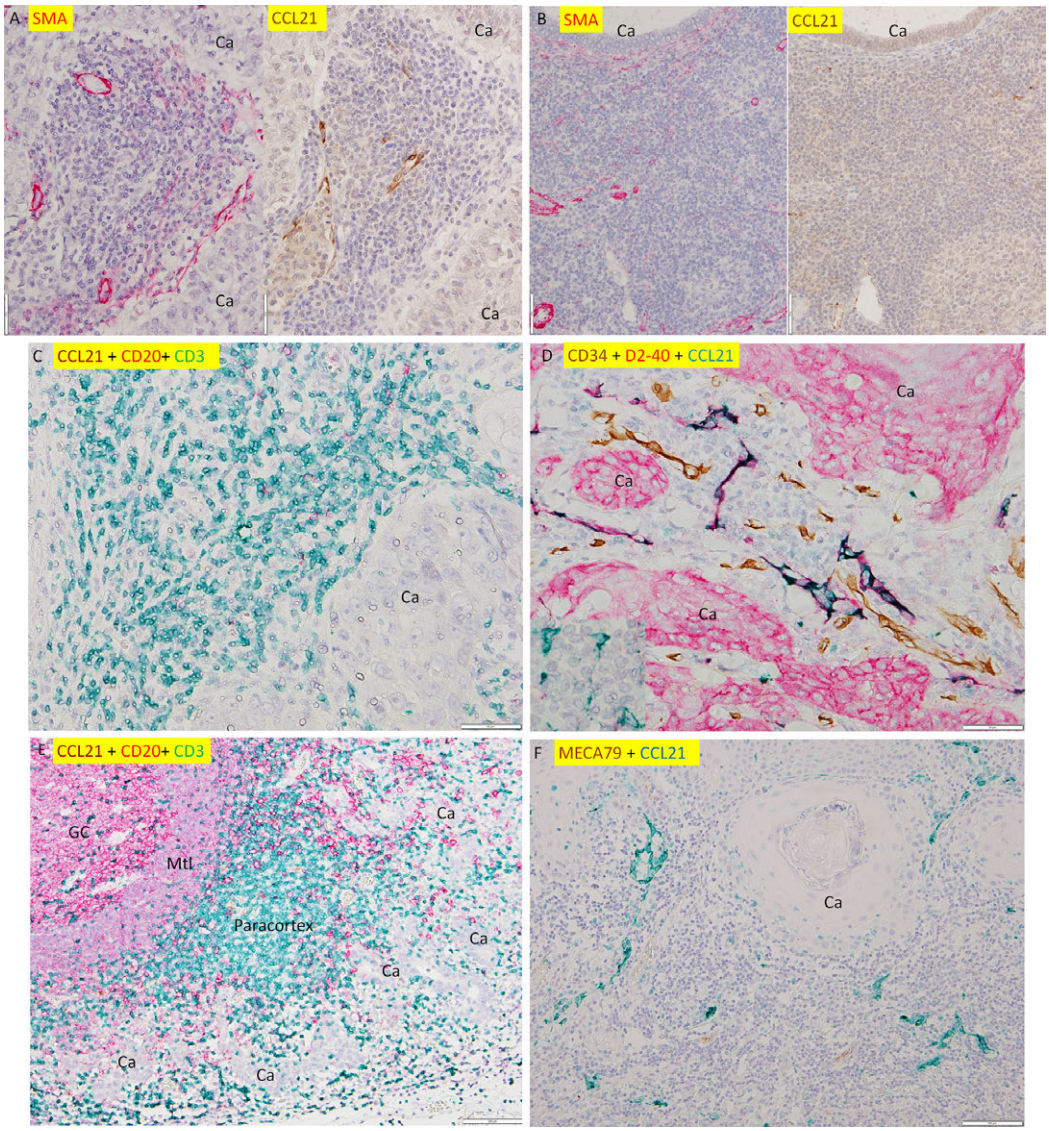

Fig. 2. Results of immunohistochemistry in carcinomas with lymphoid stroma. **A**, **B**). TCZ-FRCs are absent in lymphoid stroma of breast (**A**) and colon (**B**) carcinomas (Ca) as demonstrated by immunohistochemistry for SMA (red, left panel) and CCL21 (brown, right panel). SMA and CCL21 labels blood vessels and lymphatic vessels, respectively (refer to Fig. 1D). **C**) Triple immunohistochemistry for CCL21 (brown), CD20 (red), and CD3 (green) in carcinoma of lymphoid stroma (breast). Ca, carcinoma cells. **D**) Triple immunohistochemistry for CD34 (brown), D2-40 (red), and CCL21 (green) in skin carcinoma with lymphoid stroma. Squamous carcinoma cells (Ca) express D2-40 (red). CCL21 (green) is expressed in D2-40$^+$ lymphatic vessels (double positivity is expressed by dark blue ~ black color). CCL21$^+$ TCZ-FRCs are absent as compared with the Inset that shows CCL21$^+$ TCZ-FRCs (green) in the lymph node. **E**) Triple immunohistochemistry for CCD21 (brown), CD20 (red), and CD3 (green) in stomach carcinoma with lymphoid stroma. The germinal center (GC) with mantle zone (Mtl) is observed in the left upper corner. Juxtaposed to this, the T cell zone (paracortex) is formed (green), where CCL21$^+$ TCZ-FRCs (brown) are absent. Ca, carcinoma cells. **F**) Double immunostaining for MECA79 (brown) and CCL21 (green) in tongue carcinoma with lymphoid stroma. CCL21 is expressed in vessel structure, which is negative for MECA. MECA$^+$ vessels are not abundant. Also, note the absence of CCL21$^+$ TCZ-FRCs. Ca, carcinoma cells. Bars = 50 µm (**A**, **B**, **C**, **D**) and 100 µm (**E**, **F**).

was also observed in the normal peripheral tissues (Supplementary Fig. S2D). It was noteworthy that crescentic-shaped areas corresponding to the T cell zone (paracortex) juxtaposed with the lymphoid follicles were also devoid of TCZ-FRCs (Fig. 2E). A sporadic meshwork of TCZ-FRCs was only rarely observed in four of 30 cases (Supplementary Fig. S2E).

Double staining for MECA 79 and CCL21 (performed in 8 cases) (Fig. 2F, Supplementary Fig. S2F) confirmed the absence of CCL21$^+$ TCZ-FRCs and the infrequent occurrence of MECA 79$^+$ vessels in the cancer lymphoid stroma. As a ligand of MECA79, CD62L plays a critical role in T-cell homing to the secondary lymphoid organs [16]. Thus, this infrequent occurrence of MECA79$^+$ vessels was consistent with the infrequent CD62L$^+$ T cells in the cancer lymphoid stroma (vide infra). MECA79$^+$ vessels were mainly observed in the peripheral areas of the lymphoid stroma (Supplementary Fig. S2F)

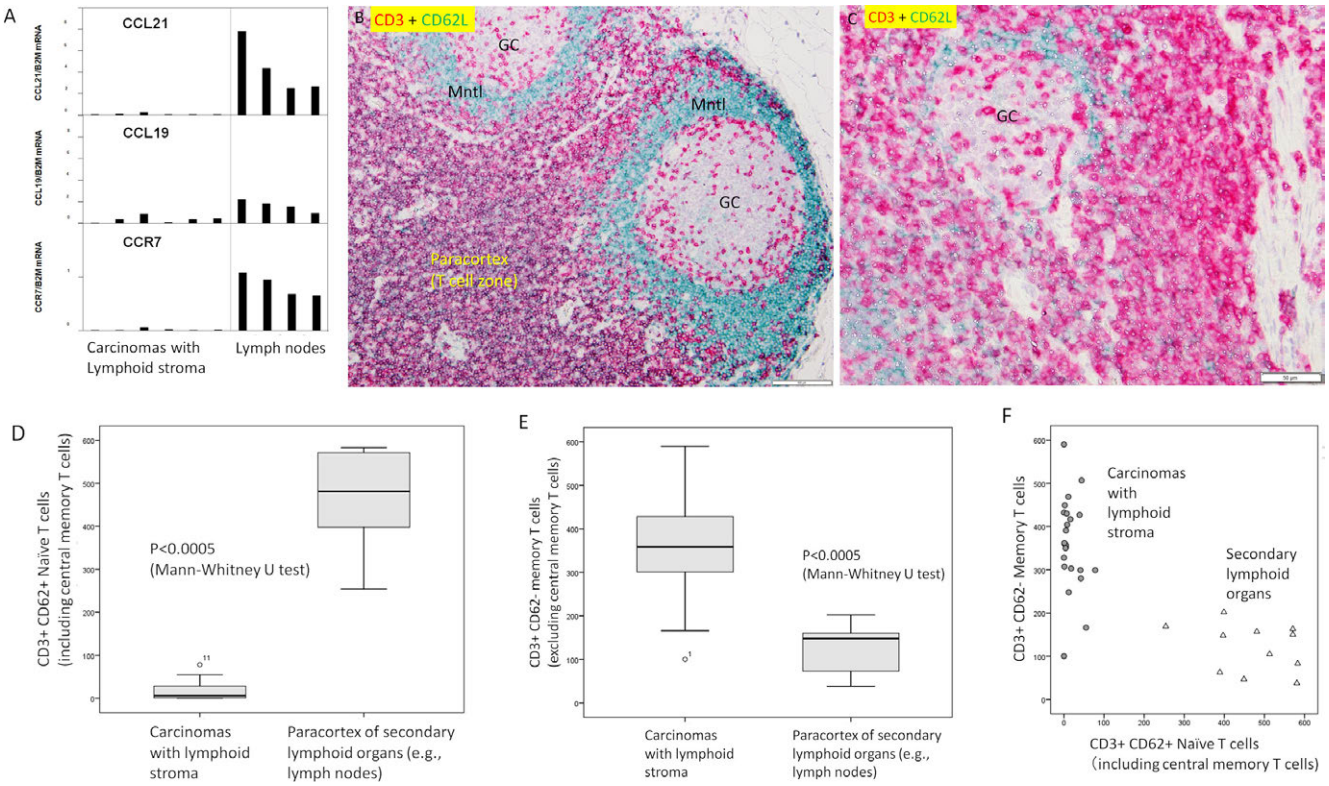

Fig. 3. Results of PCR analyses and immunohistochemistry for lymphocytes. **A**) Quantitative real-time PCR analysis confirmed that CCL21, CCL19, and CCR7 mRNAs are quite inconspicuous in cancer lymphoid stroma as compared with lymph nodes. Total RNAs were prepared from paraffin-embedded sections. The results are normalized by the expression of the β2-microglobulin gene (B2M). **B**, **C**) Double immunohistochemistry for CD3 (red) and CD62L (green) in lymph node (**B**) and colon carcinomas with lymphoid stroma (**C**). Note the affluence of $CD3^+$ $CD62L^+$ cells in the T cell zone of lymph nodes and that of $CD3^+$ $CD62L^-$ cells in cancer lymphoid stroma (colon). **D**, **E**) Morphometrical analyses confirmed that $CD3^+$ $CD62L^+$ T cells are abundant in the T cell zone of secondary lymphoid tissue (**D**), and $CD3^+$ $CD62L^-$ T cells abound in lymphoid stroma (**E**). Box-Wisker Plots. **F**) Two-dimensional scatter plots on the morphometrical analyses. Circles, carcinomas with lymphoid stroma. Triangles, secondary lymphoid organs. Bars = 100 μm (**B**) and 50 μm (**C**).

Absence of TCZ-FRCs was uniformly observed in all the 30 carcinoma cases with lymphoid stroma; i.e., histological differences (e.g., adenocarcinoma vs. squamous cell carcinoma), or difference of organs did not affect the results

mRNA analyses

To examine the mRNA expression levels of CCL21, CCL19, and their common receptor, CCR7, in cancer lymphoid stroma and lymph nodes, we performed real-time RT-PCR analyses using mRNAs extracted from FFPE sections (performed in six cancers with lymphoid stroma and four cases with lymph nodes). As illustrated in Fig. 3A, the mRNA expression levels of CCL21, CCL19, and CCR7 were lower in the cancer lymphoid stroma than in the lymph nodes.

Activation status of T-cells in cancer lymphoid stroma is different from that of the secondary lymphoid organs

The results, particularly those for CCR7, suggested a qualitative difference in lymphocytes between the two groups. Therefore, we next analyzed the T cell activation status by double immunohistochemistry for CD3 (red) and CD62L (green). CD62L is expressed in naive and central memory T lymphocytes [15, 19]. The T cell zone (paracortex) of secondary lymphoid organs (seven lymph nodes, two vermiform appendices, and two Peyer patches) exhibited an abundance of $CD3^+$ $CD62L^+$ cells (expressed by a black-like dark red color) (Fig. 3B). This was most prominent in the lymph nodes. The mantle zone was represented by pure green cells ($CD3^-$ $CD62L^+$ naïve B cells). Germinal center B cells were recognized as $CD3^-$ $CD62L^-$ cells.

In contrast, the cancer lymphoid stroma was abundant with $CD3^+$ $CD62L^-$ cells (pure red cells) representing memory-type cells (Fig. 3C). This was confirmed in 23 cases of carcinoma with lymphoid stroma of the breast (9 cases), stomach (3 cases), colon (2 cases), tongue (7 cases), and skin (2 cases). No definite accumulation of $CD3^+$ $CD62L^+$ cells (dark red cells) was observed. Morphometry confirmed these results (Fig. 3D–F).

Taken together, the cancer lymphoid stroma was different from the T cell zone of the secondary lymphoid organs, as displayed in Table 2.

Table 2. *Summary of results*

	Cancer lymphoid stroma	T cell zone (paracortex) of lymph node
Basic Structure	similar	
$CCL21^+$ TCZ-FRC	(−) absent	(+) well-developed meshwork
$MECA79^+$ HEV	(↓) only sporadic (except for peripheral area)	(+) present
T cell phenotype	mainly $CD3^+$ $CD45RO^+$ (mainly [effector] memory-type T cells)	mainly $CD3^+$ $CD45RO^-$ (mainly naïve T cells and central memory T cells)

TCZ-FRC, fibroblastic reticular cell; HEV, high endothelial venule

IV. Discussion

The present study dealt with a special variant of carcinoma, i.e., carcinomas with lymphoid stroma. Despite the heterogeneity of carcinoma cells, TCZ-FRCs were uniformly absent in cancer lymphoid stroma. Present in the T cell zone of lymph nodes TCZ-FRCs are specialized myofibroblasts that form a conduit system to transfer lymph fluid. TCZ-FRCs secrete CCL19 and CCL21, which recruit $CCR7^+$ naïve T cells so that TCZ-FRCs facilitate interactions between naïve T cells and antigen-presenting dendritic cells. Furthermore, TCZ-FRCs control the immune responses in various diseases by secreting cytokines and restricting the uncontrolled expansion of newly activated T cells [2, 4, 5]. However, TCZ-FRCs have not been widely studied in cancer except in lymph nodes with metastatic carcinomas [3, 6]. A recent report indicated that TCZ-FRCs in diffuse large B-cell lymphoma are aberrantly remodeled/activated to suppress T cell function [1]. Lymphoma is a neoplasm derived from lymphocytes. The present study is the first to analyze TCZ-FRCs in the stroma of epithelial cancer.

Lymphoid tissues formed in cancer tissues have structural similarity to secondary lymphoid organs, that is, they are well-formed tertiary lymphoid tissues/structures. The present study demonstrated that lymphoid stroma formed in cancer stroma is different from the secondary lymphoid tissue as long as TCZ-FRCs and the activation status of T cells are concerned.

In light of the aforementioned characteristics of TCZ-FRCs, our observations in the secondary lymphoid tissue are credible as the structure that retains naive T and central memory T cells. In sharp contrast, the absence of TCZ-FRCs and affluence of $CD3^+$ $CD62L^-$ cells in cancer lymphoid stroma suggest that cancer lymphoid stroma is an area of memory T cell retention (presumably effector memory T cell dominance). The results are consistent with our previous findings demonstrating abundant expression of the chemokines C-X-C motif chemokine 9 (CXCL9), CXCL10, and CXCR3 (their cognate receptors) in gastric carcinoma with lymphoid stroma [11].

We next compared our results with the tertiary lymphoid structure/tissue (TLS) formed in chronic inflammation. Manzo *et al.* described that SMA^+ $CCL21^+$ stromal cells were detected in T cell-rich area in rheumatoid arthritis, sialoadenitis in Sjögren syndrome, ulcerative colitis and Crohn's disease. They indicated that TLS in chronic inflammation was similar to the T-cell zone of secondary lymphoid organs [10]. SMA^+ $CCL21^+$ stromal cells in their report correspond to TCZ-FRCs in our study. This suggests that TLS in chronic inflammation would contain a significant amount of naïve- and central memory T-cells. In this respect, lymphoid stroma of carcinomas differs from T-cell zone of TLS formed in chronic inflammation; Cancer lymphoid stroma (well-developed TLS), which lacks TCZ-FRCs, would be abundant in more differentiated T-cells than in TLS formed in chronic inflammation.

In future studies on TLS, it is important to consider the difference between cancer lymphoid stroma and secondary lymphoid organs. Our data are confined to a specific variant of cancer with lymphoid stroma. However, focal formation of lymphoid tissue (i.e., focal formation of TLS) is commonly observed in various cancer tissues; therefore, our data are widely applicable to cancers.

In conclusion, the present study histopathologically demonstrated that the cancer lymphoid stroma is characterized by nearly complete absence of TCZ-FRCs, abounding with more activated T cells than in the T cell zone of lymph nodes. This could contribute to a better prognosis of cancer with lymphoid stroma. And the striking difference suggests that the cancer lymphoid stroma is an area of peripheral tissue with immune responses and different from lymphoid organs from the structural viewpoint.

Limitations of the present study

The present study focused on T cells, meanwhile, B cells are also important for tumor immunity [7]. We may need comparative analyses of follicular structures between the lymphoid stroma and secondary organs. The histopathological analysis of CCR7 and CCL19 expression is important. Owing to the limited availability of antibodies, we did not analyze them. Functional analyses were not performed, which are of particular importance for future studies.

V. Abbreviations

CCL, C-C motif chemokine ligand; CCR, C-C motif chemokine receptor; CD, cluster of density; DC-LAMP, dendritic cell lysosomal lysosome-associated membrane glycoprotein; FFPE, formalin-fixed, paraffin-embedded tissue; RT-qPCR, reverse transcription-quantitative polymerase chain reaction; SMA, smooth muscle actin; TCZ-

FRC, T-cell zone fibroblastic reticular cell; TLS, tertiary lymphoid structure; TIL, tumor-infiltrating lymphocyte

VI. Author Contribution

HO and ES planned the study and performed the immunohistochemical analyses. TN supervised chemokine biology. KM and KK performed RT-PCR analyses. HO drafted the manuscript, and all authors participated in the manuscript.

VII. Funding

The study was partly supported by The National Hospital Organization Collaborative Clinical Research Grants, Japan.

VIII. Data Availability

The original contributions presented are included in the article and/or supplementary data. Further inquiries can be directed to the corresponding author.

IX. Ethics Approval

The present study was approved by the Ethics Committees of Mito Saiseikai General Hospital (#H28-6) and the Mito Medical Center, and was conducted by the Declaration of Helsinki (1975).

The informed consents were replaced by the Opt-out system as indicated by the Ethics Committees.

X. Conflicts of Interest

The authors declare no conflicts of interest.

XI. Acknowledgments

We are grateful to Dr. K. Mori-Shiraishi, Dr. M. Senarita (Mito Medical Center), and Dr. T. Maruyama (Mito Siseikai General Hospital) for supplying the clinical data.

XII. References

1. Apollonio, B., Spada, F., Petrov, N., Cozzetto, D., Papazoglou, D., Jarvis, P., *et al.* (2023) Tumor-activated lymph node fibroblasts suppress T cell function in diffuse large B cell lymphoma. *J. Clin. Invest.* 133; e166070.
2. Brown, F. D. and Turley, S. J. (2015) Fibroblastic reticular cells: organization and regulation of the T lymphocyte life cycle. *J. Immunol.* 194(4); 1389–1394.
3. Eom, J., Park, S. M., Feisst, V., Chen, C. J. J., Mathy, J. E., McIntosh, J. D., *et al.* (2020) Distinctive subpopulations of stromal cells are present in human lymph nodes infiltrated with melanoma. *Cancer Immunol. Res.* 8; 990–1003.
4. Ferreira, B. O., Gamarra, L. F., Nucci, M. P., Oliveira, F. A., Rego, G. N. A. and Marti, L. (2021) LN-derived fibroblastic reticular cells and their impact on T cell response—A systematic review. *Cells* 10; 1150.
5. Fletcher, A. L., Acton, S. E. and Knoblich, K. (2015) Lymph node fibroblastic reticular cells in health and disease. *Nat. Rev. Immunol.* 15; 350–361.
6. Gao, J., Zhao, L., Liu, L., Yang, Y., Guo, B. and Zhu, B. (2017) Disrupted fibroblastic reticular cells and interleukin-7 expression in tumor draining lymph nodes. *Oncol. Lett.* 14; 2954–2960.
7. Helmink, B. A., Reddy, S, M., Gao, J., Zhang, S., Basar, R., Thakur, R., *et al.* (2020) B cells and tertiary lymphoid structures promote immunotherapy response. *Nature* 577(7791); 549–555.
8. Hendry, S., Salgado, R., Gevaert, T., Russell, P. A., John, T., Thapa, B., *et al.* (2017) Assessing tumor-infiltrating lymphocytes in solid tumors: A practical review for pathologists and proposal for a standardized method from the International Immunooncology Biomarkers Working Group: Part 1: Assessing the host immune response, TILs in invasive breast carcinoma and ductal carcinoma in situ, metastatic tumor deposits and areas for further research. *Adv. Anat. Pathol.* 24; 235–251.
9. Hendry, S., Salgado, R., Gevaert, T., Russell, P. A., John, T. and Thapa, B. (2017) Assessing tumor-infiltrating lymphocytes in solid tumors: A practical review for pathologists and proposal for a standardized method from the International Immuno-Oncology Biomarkers Working Group: Part 2: TILs in melanoma, gastrointestinal tract carcinomas, non-small cell lung carcinoma and mesothelioma, endometrial and ovarian carcinomas, squamous cell carcinoma of the head and neck, genitourinary carcinomas, and primary brain tumors. *Adv. Anat. Pathol.* 24; 311–335.
10. Manzo, A., Bugatti, S., Caporali, R., Prevo, R., Jackson, D. G., Uguccioni, M., *et al.* (2007) CCL21 expression pattern of human secondary lymphoid organ stroma is conserved in inflammatory lesions with lymphoid neogenesis. *Am. J. Pathol.* 171; 1549–1562.
11. Ohtani, H., Jin, Z., Takegawa, S., Nakayama, T. and Yoshie, O. (2009) Abundant expression of CXCL9 (MIG) by stromal cells that include dendritic cells and accumulation of CXCR3+ T cells in lymphocyte-rich gastric carcinoma. *J. Pathol.* 217; 21–31.
12. Ohtani, H. (2011) Immune Cell Responses in Gastric Carcinoma. In "Gastric Carcinoma—Molecular Aspects and Current Advances", ed. by M. Lotfy, IntechOpen, London, pp. 187–200. https://www.intechopen.com/chapters/17209
13. Ohtani, H., Mori-Shiraishi, K., Nakajima, M. and Ueki, H. (2015) Defining lymphocyte-predominant breast cancer by the proportion of lymphocyte-rich stroma and its significance in routine histopathological diagnosis. *Pathol. Int.* 65; 644–651.
14. Ohtani, H., Terashima, T. and Sato, E. (2018) Immune cell expression of TGFβ1 in cancer with lymphoid stroma: dendritic cell and regulatory T cell contact. *Virchows Arch.* 472; 1021–1028.
15. Omilusik, K. D. and Goldrath, A. W. (2019) Remembering to remember: T cell memory maintenance and plasticity. *Curr. Opin. Immunol.* 58; 89–97.
16. Rosen, S. D. (2004) Ligands for L-selectin: homing, inflammation, and beyond. *Annu. Rev. Immunol.* 22; 129–156.
17. Saiki, Y., Ohtani, H., Naito, Y., Miyazawa, M. and Nagura, H. (1996) Immunophenotypical characterization of Epstein-Barr virus-associated gastric carcinoma: Massive infiltration by proliferating CD8+ T-lymphocytes. *Lab. Invest.* 75; 67–76.
18. Salgado, R., Denkert, C., Demaria, S., Sirtaine, N., Klauschen, F., Pruneri, G., *et al.* (2015) The evaluation of tumor-infiltrating lymphocytes (TILs) in breast cancer: recommendations by an International TILs Working Group 2014. *Ann. Oncol.* 26; 259–271.

19. Sallusto, F., Geginat, J. and Lanzavecchia, A. (2004) Central memory and effector memory T cell subsets: function, generation, and maintenance. *Annu. Rev. Immunol.* 22; 745–763.
20. Sautès-Fridman, C., Petitprez, F., Calderaro, J. and Fridman, W. H. (2019) Tertiary lymphoid structures in the era of cancer immunotherapy. *Nat. Rev. Cancer* 19; 307–325.
21. Schumacher, T. N. and Thommen, D. S. (2022) Tertiary lymphoid structures in cancer. *Science* 375(6576); eabf9419.
22. Watanabe, Y., Katou, F., Ohtani, H., Nakayama, T., Yoshie, O. and Hashimoto, K. (2010) Tumor-infiltrating lymphocytes, particularly the balance between CD8(+) T cells and CCR4(+) regulatory T cells, affect the survival of patients with oral squamous cell carcinoma. *Oral Surg. Oral Med. Oral Pathol. Oral Radiol. Endod.* 109; 744–752.